Linear Response Polarizability Theory of the UV, ORD, and CD Bandshapes of Helical Biopolymers. Single- and Double-Stranded Polyadenylic Acids

Hirotoshi Ito, Yasumasa J. I'Haya, and Toshiyuki Eri

Department of Materials Science, The University of Electro-Communications, Chofu-shi, Tokyo 182

(Received November 24, 1977)

The UV, ORD, and CD spectral bandshapes of polyadenylic acid (poly A) have been investigated theoretically in order to challenge the problems of whether discrimination of the single- and double-stranded poly A's is computationally possible and of what structure poly A holds in a neutral solution. A linear response polarizability theory is applied to the derivation of UV, ORD, and CD bandshape functions of a polymer composed of N identical monomers. Using the observed and/or assumed values for the spectral bandshape of the adenine monomer, the UV, ORD, and CD spectra of both single- and double-stranded poly A's are calculated by changing geometrical parameters. The single-stranded poly A at neutral pH is assumed to have a regular helical structure which is regarded as a counterpart of the double helix form of the double-stranded poly A. This model leads to the chain-length (N) effect which in turn suggests that the structure of poly A in a neutral solution is very flexible and is such that it can be approximated as a random assembly of adenine dimers and/or trimers, when the theoretical spectra of both the single- and double-stranded poly A's are compared.

Amalgamation of the UV, ORD, and CD spectra in large molecules and molecular aggregates provides valuable information on conformation and property of the system, by which we are often able to disentangle the knots of incoherent prefiguration that has been attained from other experimental and/or theoretical sources in advance. In order to make good use of such an operation, however, a reliable theory is needed for a simultaneous analysis of these spectral bandshapes, in which working formulas for theoretical prediction of the bandshapes should be put together on an equal footing of approximations with one another. The case of helical biopolymers certainly falls under this category.

Recently, toward the analysis of the ORD and CD spectral curves of the single-stranded polyadenylic acid (poly A), we have demonstrated the promising reliability and wide applicability of the linear response polarizability theory[1] which is essentially a unified theory of the Fano-DeVoe model[2-5] with Applequist's polarizability theory of optical rotation[6]. As a closely equivalent treatment to ours, Cech *et al.*[7] have shown that DeVoe's all-orders-coupled oscillator polarizability model[3,4] successfully reproduces the CD spectrum of poly A. However, in contrast to such an extensive application of DeVoe's model, we like to point out that our model for the UV, ORD, and CD spectral bandshapes has a more convenient merit in correlating and explaining the molecular properties of biopolymers in terms of a small number of parameters; *i.e.*, transition energies, oscillator strengths, directions of transition moments, and half-widths of the absorption spectra of constituent monomer molecules.

The observed ORD and CD spectra of poly A are entirely different in acid (pH 4.6) and neutral solutions, indicating the existence of conformations of different kinds.[8-10] Optical absorption spectra,[8,10] viscosity measurement,[8] and X-ray analysis[11] offer an evidence that poly A shapes into the single-stranded helix in neutral solution and into the double-stranded helix in low pH solution, at room temperature. A possible explanation for such difference in conformation is a matter of main concern in the present paper. We therefore carry out comparative calculations of the UV, ORD, and CD spectral bandshapes of poly A by making use of the linear response theory, and show how the molecular conformations are reflected in these spectral bandshapes computed by varying the necessary molecular geometrical parameters. Afterward, we will discuss a problem of whether the discrimination of the single- and double-stranded poly A's can be made on the basis of the theoretical prediction of spectral bandshapes.

In the following, we first define a polarizability tensor of a homopolymer, and next outline the derivation of the UV, ORD, and CD bandshape functions by making use of the polarizability tensor. We then mention the geometrical properties of a helical polymer, by which we compute the bandshapes under a variety of conditions.

Polymer Polarizability Tensor

Let us consider the matrix elements of the polarizability tensor, $\boldsymbol{\alpha}^{P}_{mn}(\tilde{\nu})$, of a polymer composed of N identical monomers (N-mer). The polymer polarizability tensor can be bulit up from the polarizability tensors, $\boldsymbol{\alpha}^{M}_{mn}(\tilde{\nu})$, of individual monomers by making use of the Green's function method, when we know the unperturbed monomer polarizability tensor,

$$\begin{aligned}\boldsymbol{\alpha}^{M}_{mn}(\tilde{\nu}) &= \boldsymbol{\alpha}^{M}_{mn}(\tilde{\nu})\delta_{mn} = \boldsymbol{\alpha}^{M}_{m}(\tilde{\nu}) \\ &= +(hc)^{-1}\sum_{\lambda}\boldsymbol{\mu}^{(m)}_{0\lambda}\boldsymbol{\mu}^{(m)}_{\lambda 0}[(\tilde{\nu}-\tilde{\nu}^{(m)}_{\lambda 0}+i\eta_{\lambda})^{-1} \\ &\qquad -(\tilde{\nu}+\tilde{\nu}^{(m)}_{\lambda 0}-i\eta_{\lambda})^{-1}], \qquad (1)\end{aligned}$$

where

$$\boldsymbol{\mu}^{(m)}_{0\lambda} = \langle 0^{(m)}|\sum_{i} e(\mathbf{r}_i-\mathbf{r}_m)|\lambda^{(m)}\rangle \equiv \langle 0^{(m)}|\boldsymbol{\mu}_m|\lambda^{(m)}\rangle. \qquad (2)$$

$\boldsymbol{\mu}^{(m)}_{0\lambda}\boldsymbol{\mu}^{(m)}_{\lambda 0}$ is a dyadic product of the transition moment between the λth excited state $|\lambda^{(m)}\rangle$ and the ground state $|0^{(m)}\rangle$ of the mth monomer; $\mathbf{r}_i$ and $\mathbf{r}_m$ are the vectors going from the origin of the system to the ith electron of the mth monomer and to the center of the mth monomer, respectively; η_{λ} is a positive and infinitesimally small quantity. $\boldsymbol{\alpha}^{M}_{m}(\tilde{\nu})$ is given in units of cm^3 when $(\boldsymbol{\mu}^{(m)}_{\lambda 0}/e)$ is measured in units of cm, $\tilde{\nu}$ is in units of cm^{-1}, and $e^2/(hc)=1.1614093\times10^{-3}$. Note

that the plus sign before $(hc)^{-1}$ of Eq. 1 defines the sign convention for the polarizability adopted in the present paper, which is different from the usual one. Hereafter, the superscripts, (1), (2), ···, denote the successive numbers of residues.

In the treatment mentioned above, the excited states of the polymer system is actually regarded as perturbed excited states of a hypothetically non-interacting molecular aggregate of N identical monomers, which are created by the intermolecular Coulomb interaction upon excitation. We do not consider the intermolecular exchange of electrons. Now, let us calculate the Coulomb interaction V_{mn} between the mth and nth monomers by the dipole-dipole approximation. It is then convenient to expand the Coulomb interaction V_{mn} in terms of the dipole operators $\boldsymbol{\mu}_m$ and $\boldsymbol{\mu}_n$ and the unit dipole interaction tensor $\mathbf{U}_{mn}$;

$$V_{mn} = \sum_{i\in m}\sum_{j\in n}(e^2/r_{ij}) \approx \sum_i e(\mathbf{r}_i-\mathbf{r}_m)\cdot\mathbf{U}_{mn}\cdot\sum_j e(\mathbf{r}_j-\mathbf{r}_n) = \boldsymbol{\mu}_m\cdot\mathbf{U}_{mn}\cdot\boldsymbol{\mu}'_n. \tag{3}$$

Instead, we use the following notation for V_{mn} hereafter;

$$\{V(\mathbf{r},\mathbf{r}')\}_{mn} \approx e(\mathbf{r}-\mathbf{r}_m)\cdot\mathbf{U}_{mn}\cdot e(\mathbf{r}'-\mathbf{r}'_n), \tag{4}$$

where

$$\mathbf{U}_{mn} = (1/r_{mn}^3)(\mathbf{1}_{mn}-3\mathbf{r}_{mn}\mathbf{r}_{mn}/r_{mn}^2) = -(3/r_{mn}^5)\begin{pmatrix} x_{mn}^2-(r_{mn}^2/3) & x_{mn}y_{mn} & x_{mn}z_{mn} \\ y_{mn}x_{mn} & y_{mn}^2-(r_{mn}^2/3) & y_{mn}z_{mn} \\ z_{mn}x_{mn} & z_{mn}y_{mn} & z_{mn}^2-(r_{mn}^2/3)\end{pmatrix}. \tag{5}$$

In Eqs. 3 and 4, the single dot denotes the single contraction and $\mathbf{r}_{mn}$ is a vector for intermolecular distance,

$$\mathbf{r}_{mn} = \mathbf{r}_n - \mathbf{r}_m = x_{mn}\hat{\mathbf{i}} + y_{mn}\hat{\mathbf{j}} + z_{mn}\hat{\mathbf{k}}. \tag{6}$$

The polarizability tensor is derived from the polarization propagator[5] $G(\mathbf{r},\mathbf{r}';E)$, which describes the propagation of the electronic density fluctuation, the propagator of the mth monomer being given by

$$G_m^{\mathrm{M}}(\mathbf{r},\mathbf{r}';E) = G_{mn}^{\mathrm{M}}(\mathbf{r},\mathbf{r}';E)\delta_{mn} = \sum_\lambda\left(\frac{\langle 0^{(m)}|\rho(\mathbf{r})|\lambda^{(m)}\rangle\langle\lambda^{(m)}|\rho(\mathbf{r}')|0^{(m)}\rangle}{E-E_{\lambda 0}^{(m)}+i\eta_\lambda} - \frac{\langle 0^{(m)}|\rho(\mathbf{r}')|\lambda^{(m)}\rangle\langle\lambda^{(m)}|\rho(\mathbf{r})|0^{(m)}\rangle}{E+E_{\lambda 0}^{(m)}-i\eta_\lambda}\right)\delta_{mn}, \tag{7}$$

with

$$\rho(\mathbf{r}) = \sum_i \delta([\mathbf{r}-\mathbf{r}_m]-\mathbf{r}_i), \qquad \rho(\mathbf{r}') = \sum_i \delta([\mathbf{r}'-\mathbf{r}_n]-\mathbf{r}_i), \tag{8}$$

where $E=hc\tilde{\nu}$ and $E_{\lambda 0}^{(m)}=hc\tilde{\nu}_{\lambda 0}^{(m)}$.

The electronic density disturbance and fluctuation induced by the external light source are accompanied with the transition dipole moment, the measure of which defines the polarizability. Then, the monomer polarizability tensor can naturally be defined by

$$\boldsymbol{\alpha}_{mn}^{\mathrm{M}}(E) = \int_m \mathrm{d}^3\mathbf{r}\int_n \mathrm{d}^3\mathbf{r}' e(\mathbf{r}-\mathbf{r}_m)G_{mn}^{\mathrm{M}}(\mathbf{r},\mathbf{r}';E)e(\mathbf{r}'-\mathbf{r}'_n), \tag{9}$$

where m and n close by the integral signs denote the integration only over such domains that $\mathbf{r}$ and $\mathbf{r}'$ lie in the mth and nth monomers, respectively. From Eq. 7, $\langle 0^{(m)}|\rho(r)|\lambda^{(m)}\rangle$ is obviously found to be the transition density, so that Eq. 2 is rewritten as

$$\boldsymbol{\mu}_{0\lambda}^{(m)} = \int \mathrm{d}^3\mathbf{r} e(\mathbf{r}-\mathbf{r}_m)\langle 0^{(m)}|\rho(\mathbf{r})|\lambda^{(m)}\rangle. \tag{10}$$

In the zeroth order, the polarization propagator for the polymer is hypothetically assumed to be

$$\{G^{\mathrm{HP}}(\mathbf{r},\mathbf{r}';E)\}_{mn} = G_m^{\mathrm{M}}(\mathbf{r},\mathbf{r}';E)\delta_{mn}. \tag{11}$$

It is then preferable to write down the higher order terms in the following manner:[5]

$$G^{\mathrm{P}}(\mathbf{r},\mathbf{r}';E) = G^{\mathrm{HP}}(\mathbf{r},\mathbf{r}';E) + \int \mathrm{d}^3\mathbf{r}''\int \mathrm{d}^3\mathbf{r}''' G^{\mathrm{HP}}(\mathbf{r},\mathbf{r}'';E)V(\mathbf{r}'',\mathbf{r}''')G^{\mathrm{P}}(\mathbf{r}''',\mathbf{r}';E), \tag{12}$$

or in its matrix element representation,

$$G_{mn}^{\mathrm{P}}(\mathbf{r},\mathbf{r}';E) = G_m^{\mathrm{M}}(\mathbf{r},\mathbf{r}';E)\delta_{mn} + \int_m \mathrm{d}^3\mathbf{r}''\int_n \mathrm{d}^3\mathbf{r}''' G_m^{\mathrm{M}}(\mathbf{r},\mathbf{r}'';E)\{V(\mathbf{r}'',\mathbf{r}''')\}_{mn}\cdot G_n^{\mathrm{M}}(\mathbf{r}''',\mathbf{r}';E) + \cdots \tag{13}$$

Finally, we have the following expression for the polymer polarizability tensor:

$$\boldsymbol{\alpha}_{mn}^{\mathrm{P}}(\tilde{\nu}) = \int_m \mathrm{d}^3\mathbf{r}\int_n \mathrm{d}^3\mathbf{r}' e(\mathbf{r}-\mathbf{r}_m)G_{mn}^{\mathrm{P}}(\mathbf{r},\mathbf{r}';hc\tilde{\nu})e(\mathbf{r}'-\mathbf{r}'_n) = \boldsymbol{\alpha}_m^{\mathrm{M}}(\tilde{\nu})\delta_{mn} + \boldsymbol{\alpha}_m^{\mathrm{M}}(\tilde{\nu})\cdot\mathbf{U}_{mn}\cdot\boldsymbol{\alpha}_n^{\mathrm{M}}(\tilde{\nu}) + \sum_l \boldsymbol{\alpha}_m^{\mathrm{M}}(\tilde{\nu})\cdot\mathbf{U}_{ml}\cdot\boldsymbol{\alpha}_l^{\mathrm{M}}(\tilde{\nu})\cdot\mathbf{U}_{ln}\cdot\boldsymbol{\alpha}_n^{\mathrm{M}}(\tilde{\nu}) + \cdots \tag{14}$$

UV, ORD, and CD Bandshape Functions of an N-mer

In the present paper, optical rotation of a helical polymer is ragarded as optical rotation induced conformationally by the regular aggregation of achiral residues in the absorption region of the residues. This means that the optical activity is derived from the electronic interaction among the achiral residues. In fact, it is known that the magnitudes of conformationally induced optical rotation of natural and synthetic polynucleotides are much larger than those of intrinsic optical rotation of isolated mononucleotides having chrial structures.[8] In order to predict optical activity of polynucleotides in the present formalism, chiral residues such as mononucleotides can therefore be approximated by achiral residues such as nucleic acid bases, neglecting the sugar-phosphate backbones. In the following, we also derive a scalar representation for the polarizability of such polymers, which is rather convenient for practical computations of UV spectral bandshapes compared with Eq. 14.

The total dipole moment of the polymer induced by the applied external field $\mathbf{E}(\mathbf{r}_n)$ is given by

$$\boldsymbol{\mu}^{\mathrm{P}}(\tilde{\nu}) = \sum_m^N \boldsymbol{\mu}_m^{\mathrm{P}}(\tilde{\nu}) = \sum_m^N\sum_n^N \boldsymbol{\alpha}_{mn}^{\mathrm{P}}(\tilde{\nu})\cdot\mathbf{E}(\mathbf{r}_n) = \sum_m^N\sum_n^N \boldsymbol{\alpha}_{mn}^{\mathrm{P}}(\tilde{\nu})\cdot[\mathbf{E}(0)+\mathbf{r}_n\cdot\nabla\mathbf{E}(0)], \tag{15}$$

where the second line is obtained by Taylor's expansion of $\mathbf{E}(\mathbf{r}_n)$ about the origin of the polymer coordinate system. Taking the average over all orientations with

respect to the laboratory-fixed coordinate system, we obtain the following relationship, which is the same as that derived by Applequist:[6]

$$\langle \boldsymbol{\mu}^{\mathrm{P}}(\tilde{\nu})\rangle_{\mathrm{av}} = (1/3)\sum_{m}^{\mathrm{N}}\sum_{n}^{\mathrm{N}}[\mathrm{tr}\,\boldsymbol{\alpha}^{\mathrm{P}}_{mn}(\tilde{\nu})]\mathbf{E}(0) + (1/6)\sum_{m}^{\mathrm{N}}\sum_{n}^{\mathrm{N}}\mathbf{r}_n\cdot(\boldsymbol{\alpha}^{\mathrm{P}}_{mn}(\tilde{\nu}):\boldsymbol{\varepsilon})\nabla\times\mathbf{E}(0) = \sum_{m}^{\mathrm{N}}\sum_{n}^{\mathrm{N}}\bar{\alpha}^{\mathrm{P}}_{mn}(\tilde{\nu})\mathbf{E}(0) + \beta(\tilde{\nu})\,\mathrm{Rot}\,\mathbf{E}(0), \quad (16)$$

where $\boldsymbol{\varepsilon}$ is the isotropic third order tensor. The double-dot product of the two tensors in the parentheses reduces to

$$\boldsymbol{\alpha}^{\mathrm{P}}_{mn}(\tilde{\nu}):\boldsymbol{\varepsilon} = [\alpha^{\mathrm{Pzy}}_{mn}-\alpha^{\mathrm{Pyz}}_{mn}]\hat{\mathbf{i}} + [\alpha^{\mathrm{Pxz}}_{mn}-\alpha^{\mathrm{Pzx}}_{mn}]\hat{\mathbf{j}} + [\alpha^{\mathrm{Pyx}}_{mn}-\alpha^{\mathrm{Pxy}}_{mn}]\hat{\mathbf{k}}, \quad (17)$$

where the superscripts zy, yz, *etc.* indicate the tensor components. $\bar{\alpha}^{\mathrm{P}}_{mn}(\tilde{\nu})$ in the second line of Eq. 16 defines the scalar polarizability of the polymer. The coefficient before Rot $\mathbf{E}(0)$ in Eq. 16 is the molecular rotatory parameter $\beta(\nu)$ which measures the rotation of the electric field vector of the light wave passing through the medium at the point $\mathbf{r}_n$ measured from the origin;

$$\begin{aligned}\beta(\tilde{\nu}) &= (1/6)\sum_{m}^{\mathrm{N}}\sum_{n}^{\mathrm{N}}\mathbf{r}_n\cdot(\boldsymbol{\alpha}^{\mathrm{P}}_{mn}(\tilde{\nu}):\boldsymbol{\varepsilon})\\ &= -(1/6)\sum_{m}^{\mathrm{N}}\sum_{n}^{\mathrm{N}}\mathbf{r}_m\cdot(\boldsymbol{\alpha}^{\mathrm{P}}_{mn}(\tilde{\nu}):\boldsymbol{\varepsilon})\\ &= (1/12)\sum_{m}^{\mathrm{N}}\sum_{n}^{\mathrm{N}}\mathbf{r}_{mn}\cdot(\boldsymbol{\alpha}^{\mathrm{P}}_{mn}(\tilde{\nu}):\boldsymbol{\varepsilon})\\ &= (1/12)\sum_{m}^{\mathrm{N}}\sum_{n}^{\mathrm{N}}\{x_{mn}(\alpha^{\mathrm{Pzy}}_{mn}(\tilde{\nu})-\alpha^{\mathrm{Pyz}}_{mn}(\tilde{\nu}))\\ &\qquad + y_{mn}(\alpha^{\mathrm{Pxz}}_{mn}(\tilde{\nu})-\alpha^{\mathrm{Pzx}}_{mn}(\tilde{\nu}))\\ &\qquad + z_{mn}(\alpha^{\mathrm{Pyx}}_{mn}(\tilde{\nu})-\alpha^{\mathrm{Pxy}}_{mn}(\tilde{\nu}))\}. \end{aligned} \quad (18)$$

Here, it should be noticed that in the third line the factor (1/2) is introduced by combining the first line with the second one. The minus sign before the second line follows from Eq. 17, by interchanging suffixes m and n and also by allowing for the fact that $\boldsymbol{\alpha}^{\mathrm{P}}_{mn}$ is equal to the transposed element of $\boldsymbol{\alpha}^{\mathrm{P}}_{mn}$.

By relating β to the macroscopic quantities, molar rotation and ellipticity,[1] one obtains the bandshape functions $[\Psi(\tilde{\nu})]$ and $[\Xi(\tilde{\nu})]$ of the ORD and CD spectra, respectively;

$$[\Psi(\tilde{\nu})] = -288\pi^2 N_{\mathrm{A}}\tilde{\nu}^2(1/N)\,\mathrm{Re}\,\beta(\tilde{\nu}) \quad (\mathrm{deg\,cm^2\,dmol^{-1}}), \quad (19)$$

$$[\Xi(\tilde{\nu})] = -288\pi^2 N_{\mathrm{A}}\tilde{\nu}^2(1/N)\,\mathrm{Im}\,\beta(\tilde{\nu}) \quad (\mathrm{deg\,cm^2\,dmol^{-1}}), \quad (20)$$

where N_{A} is Avogadro's number.

The bandshape function of the UV absorption spectrum is derived from the coefficient of $\mathbf{E}(0)$ in the first term of Eq. 16. The wave number-dependent molar extinction coefficient[12] is then computed by

$$\varepsilon(\tilde{\nu}) = -(8\pi^2 N_{\mathrm{A}}/2302.6)\tilde{\nu}[(1/N)\sum_{m}^{\mathrm{N}}\sum_{n}^{\mathrm{N}}\mathrm{Im}\,\bar{\alpha}^{\mathrm{P}}_{mn}(\tilde{\nu})], \quad (\mathrm{l\,mol^{-1}\,cm^{-1}}). \quad (21)$$

Note that the factor (1/3) is involved in $\bar{\alpha}^{\mathrm{P}}_{mn}(\tilde{\nu})$.

For a model polymer composed of translationally and/or helically arranged equivalent monomers,[13] neglecting an end effect, we can derive

$$\sum_{m}^{\mathrm{N}}\sum_{n}^{\mathrm{N}}\bar{\alpha}^{\mathrm{P}}_{mn}(\tilde{\nu}) = (1-\sum_{m}^{\mathrm{N}}\bar{U}_{nm}\bar{\alpha}^{\mathrm{M}}_{n}(\tilde{\nu}))^{-1}\sum_{m}^{\mathrm{N}}\sum_{n}^{\mathrm{N}}\bar{\alpha}^{\mathrm{M}}_{n}(\tilde{\nu})\delta_{nm} = N\bar{\alpha}^{\mathrm{M}}_{n}(\tilde{\nu})(1-\sum_{m}^{\mathrm{N}}\bar{U}_{nm}\bar{\alpha}^{\mathrm{M}}_{m}(\tilde{\nu}))^{-1}, \quad (22)$$

which involves the dipole-dipole interactions to infinite orders. $\bar{U}_{nm}$ is the scalar interaction potential between unit dipoles,

$$\bar{U}_{nm} = \mathbf{e}_n\cdot\mathbf{e}_m/r^3_{nm} - 3(\mathbf{e}_n\cdot\mathbf{r}_{nm})(\mathbf{e}_m\cdot\mathbf{r}_{nm})/r^5_{nm}, \quad (23)$$

where the unit vector $\mathbf{e}_m$ is defined by

$$\boldsymbol{\mu}^{(m)}_{0\lambda} = |\boldsymbol{\mu}^{(m)}_{0\lambda}|\mathbf{e}_m. \quad (24)$$

Equation 22 is a scalar representation for the polymer polarizability, which is convenient for the evaluation of UV spectral bandshapes. However, we do not employ Eq. 22 in actual computations, because we want to compute UV, ORD, and CD bandshapes altogether on the same approximate grounds. Therefore, we use Eq. 14, in which terms higher than the third terms are truncated, for all the bandshape calculations.

For the calculations of Eqs. 19—21, which reduce to those of the real and imaginary parts of $\boldsymbol{\alpha}^{\mathrm{M}}_{m}(\tilde{\nu})$, the necessary formulas[1,13] are obtained as follows:

$$\begin{aligned}\mathrm{Im}\,\boldsymbol{\alpha}^{\mathrm{M}}_{m}(\tilde{\nu}) &= -\pi(hc)^{-1}\sum_{\lambda}\boldsymbol{\mu}^{(m)}_{0\lambda}\boldsymbol{\mu}^{(m)}_{\lambda 0}\{\delta(\tilde{\nu}-\tilde{\nu}^{(m)}_{\lambda 0}) + \delta(\tilde{\nu}+\tilde{\nu}^{(m)}_{\lambda 0})\}\\ &= -(hc)^{-1}\sum_{\lambda}\boldsymbol{\mu}^{(m)}_{0\lambda}\boldsymbol{\mu}^{(m)}_{\lambda 0}\{\eta_\lambda[(\tilde{\nu}-\tilde{\nu}^{(m)}_{\lambda 0})^2+\eta^2_\lambda]^{-1}\\ &\qquad +\eta_\lambda[(\tilde{\nu}+\tilde{\nu}^{(m)}_{\lambda 0})^2+\eta^2_\lambda]^{-1}\}, \end{aligned} \quad (25)$$

and

$$\begin{aligned}\mathrm{Re}\,\boldsymbol{\alpha}^{\mathrm{M}}_{m}(\tilde{\nu}) &= -(\mathcal{P}/\pi)\int_{-\infty}^{\infty}\mathrm{d}E\,\mathrm{Im}\,\boldsymbol{\alpha}^{\mathrm{M}}_{m}(E)\,\mathrm{sign}\,(E)(\tilde{\nu}-E)^{-1}\\ &= +(hc)^{-1}\sum_{\lambda}\boldsymbol{\mu}^{(m)}_{0\lambda}\boldsymbol{\mu}^{(m)}_{\lambda 0}\{(\tilde{\nu}-\tilde{\nu}^{(m)}_{\lambda 0})[(\tilde{\nu}-\tilde{\nu}^{(m)}_{\lambda 0})^2+\eta^2_\lambda]^{-1}\\ &\qquad -(\tilde{\nu}+\tilde{\nu}^{(m)}_{\lambda 0})[(\tilde{\nu}+\tilde{\nu}^{(m)}_{\lambda 0})^2+\eta^2_\lambda]^{-1}\}, \end{aligned} \quad (26)$$

both of which represent features of the Lorentzian bandshape.

In this computation, the damping factor $\eta_\lambda = (1/2)$ (half-width) is treated as an empirical parameter, with the condition $\eta_\lambda \ll \tilde{\nu}^{(m)}_{\lambda 0}$. From Eqs. 21 and 25, we can derive the approximate working formula for estimating η_λ (in $\mathrm{cm^{-1}}$) from the experimental values for the molar extinction coefficient ε^{M} and the oscillator strength $f_{\lambda 0}$ of the monomer molecule;

$$[\varepsilon^{\mathrm{M}}(\tilde{\nu}^{(m)}_{\lambda 0})]_{\max} \approx 7.37126\times 10^7(f_{\lambda 0}/\eta_\lambda), \quad (27)$$

when the second term of Eq. 25 is neglected (this is justified because the second term is usually much smaller than the first term in Eq. 25). By substituting these approximate η_λ's into Eqs. 25 and 26, real and imaginary parts of the monomer polarizability tensor are computed.

It should finally be noted that the sum rule[1,13] holds for the UV, ORD, and CD spectral intensities. In the present scheme, it is clearly understood that the total polarizability tensor given in Eq. 14 for the conformationally induced optically active polymer becomes a 3×3 antisymmetric matrix which is derived from the monomer 3×3 (diagonal and/or symmetric) polariz-

ability tensors. In other words, the absorption spectrum is given by the diagonal terms of the polymer polarizability tensor, while the optical activity is determined by the off-diagonal terms.

Geometrical Properties for a Helical Polymer

In the computational work, it is necessary to know the geometrical properties of the regular polymers such as single- and double-stranded poly A's.

(i) For a single-stranded helical homopolymer, let the origin of the whole system be the center of the circle cut off perpendicularly to the helix axis, in which the center of one of the monomers (called the first monomer) is involved. The unit vector $\hat{\mathbf{i}}$ is taken perpendicularly to the helix axis to the center of the first monomer (radial), $\hat{\mathbf{j}}$ perpendicular to $\hat{\mathbf{i}}$ (tangential to the helix), both in the plane of the section, and $\hat{\mathbf{k}}$ along the helix axis (Figs. 1 and 2). Then the vector $\mathbf{r}_n$ going from the origin to the center of the nth monomer is expressed by

$$\mathbf{r}_n = a\cos(n\phi)\hat{\mathbf{i}} + a\sin(n\phi)\hat{\mathbf{j}} + nL\hat{\mathbf{k}}, \tag{28}$$

where a is the radius of the sectional circule, L the pitch of the helix (the advance parallel to the helix axis), and ϕ is the angle of rotation transferring a given monomer, n say, to the next nearest one, $n+1$. The distance vector between the mth and nth monomers is then defined by Eq. 6. By making use of the rotational operator, $\mathbf{R}((n-1)\phi)$, we can relate the polarizability tensor of the nth monomer to that of the first monomer;

$$\boldsymbol{\alpha}_n^{\mathrm{M}}(\tilde{\nu}) = \mathbf{R}((n-1)\phi)\cdot\boldsymbol{\alpha}_1^{\mathrm{M}}(\tilde{\nu})\cdot\mathbf{R}(-(n-1)\phi), \tag{29}$$

since

$$\boldsymbol{\mu}_{0\lambda}^{(n)} = [\mathbf{R}(\phi)]^{n-1}\cdot\boldsymbol{\mu}_{0\lambda}^{(1)} = \mathbf{R}((n-1)\phi)\cdot\boldsymbol{\mu}_{0\lambda}^{(1)} \equiv \begin{pmatrix} \cos((n-1)\phi) & -\sin((n-1)\phi) & 0 \\ \sin((n-1)\phi) & \cos((n-1)\phi) & 0 \\ 0 & 0 & 1 \end{pmatrix} \begin{pmatrix} [\mu_{0\lambda}^{(1)}]_{\hat{\mathbf{i}}} \\ [\mu_{0\lambda}^{(1)}]_{\hat{\mathbf{j}}} \\ [\mu_{0\lambda}^{(1)}]_{\hat{\mathbf{k}}} \end{pmatrix}, \tag{30}$$

where $[\boldsymbol{\mu}_{0\lambda}^{(1)}]_{\hat{\mathbf{i}}}$ *etc.* are the components of the transition moment of the first monomer in the directions of $\hat{\mathbf{i}}$ (ridial), $\hat{\mathbf{j}}$ (tangential), and $\hat{\mathbf{k}}$ fixed as the center of the first monomer.

(ii) For a double-stranded helical homopolymer like (poly A)·(poly A), we assign the odd integers $\{2m'-1, 2n'-1\}$ for the numberings of the positions of the residues (placed in the x'y'-plane of Fig. 3 or displaced translationally along the helix axis) in one of the strands and the even numbers {2m', 2n'} for those (in the x"y"-plane) in another strand.

Let us obtain the intermolecular distances in the double-stranded polymers. The position vectors for the double-strands are now given by

$$\mathbf{r}_{2m'-1} = a\cos(m'\phi)\hat{\mathbf{i}} + a\sin(m'\phi)\hat{\mathbf{j}} + m'L\hat{\mathbf{k}}, \tag{31}$$

$$\mathbf{r}_{2m'} = a\cos(m'\phi+\gamma')\hat{\mathbf{i}} + a\sin(m'\phi+\gamma')\hat{\mathbf{j}} + (m'L+L')\hat{\mathbf{k}}, \tag{32}$$

where a translation L' along the helix axis followed by

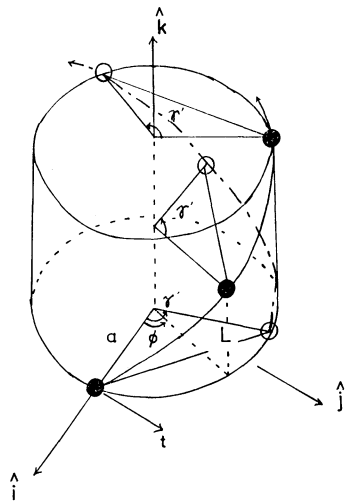

Fig. 1. Double-stranded helix and its geometrical parameters (a, ϕ, L, γ', L'). Solid circles represent the residues on one of the strands and open circles those on the other strand. $\hat{\mathbf{i}}$, $\hat{\mathbf{j}}$ and $\hat{\mathbf{k}}$ are the unit vectors in the Cartesian coordinate, $\hat{\mathbf{k}}$ being along the helical axis.

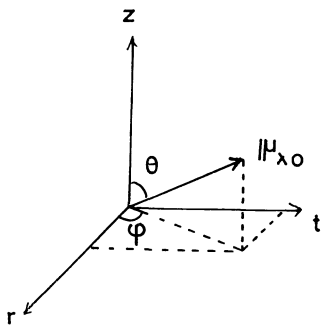

Fig. 2. Coordinate system for transition moment of a residue. r is the radial direction and t is tangential to the helix, z being along the helical axis.

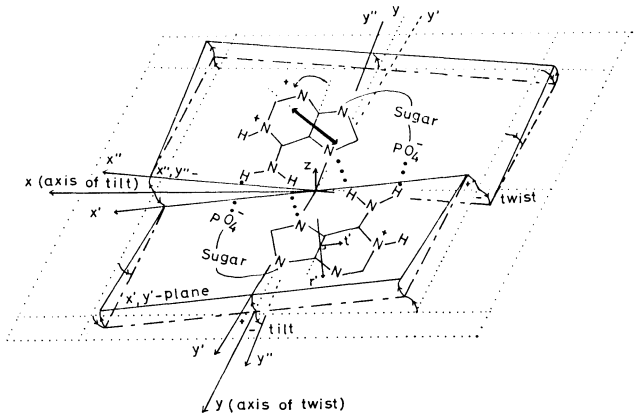

Fig. 3. Perspective drawing of a hydrogen-bonded base pair in the double-stranded polyadenylic acid. The bold arrow represents the direction of the transition moment. r' and t' are, respectively, the radial and tangential directions of the residue on the x',y'-plane. As for the other notations, see the text.

a rotation γ' about the axis brings about either of strands onto another strand as shown in Fig. 1. The vector for the intermolecular distance is again calculated from Eq. 6.

The following relationships produced by the screw operation in this polymer system also make it easy to carry out the actual computation. For one of the strands, we can relate the $(2n'+1)$th monomer with the first monomer in the following manner:

$$\boldsymbol{\mu}_{0\lambda}^{(2n'+1)} = \mathbf{R}(n'\phi)\cdot\boldsymbol{\mu}_{0\lambda}^{(1)}, \tag{33}$$

$$\boldsymbol{\alpha}_{2m'+1,2n'+1}^{M}(\tilde{\nu}) = \mathbf{R}(m'\phi)\cdot\boldsymbol{\alpha}_{11}^{M}(\tilde{\nu})\cdot\mathbf{R}(-n'\phi). \tag{34}$$

For the other strand, we also have similar relationships;

$$\boldsymbol{\mu}_{0\lambda}^{(2n'+2)} = \mathbf{R}(n'\phi)\cdot\boldsymbol{\mu}_{0\lambda}^{(2)}, \tag{35}$$

$$\boldsymbol{\alpha}_{2m'+2,2n'+2}^{M}(\tilde{\nu}) = \mathbf{R}(m'\phi)\cdot\boldsymbol{\alpha}_{22}^{M}(\tilde{\nu})\cdot\mathbf{R}(-n'\phi). \tag{36}$$

From Eqs. 34 and 36, we can derive

$$\boldsymbol{\alpha}_{2m'+2,2n'+2}^{M}(\tilde{\nu}) = \mathbf{R}(\gamma')\cdot\boldsymbol{\alpha}_{2m'+1,2n'+1}^{M}(\tilde{\nu})\cdot\mathbf{R}(-\gamma'), \tag{37}$$

since

$$\boldsymbol{\mu}_{0\lambda}^{(2)} = \mathbf{R}(\gamma')\cdot\boldsymbol{\mu}_{0\lambda}^{(1)} \equiv \mathbf{R}_z(-\gamma')\cdot\boldsymbol{\mu}_{0\lambda}^{(1)}, \tag{38}$$

where $\mathbf{R}_z$ denotes an operator defined by the rotation of the coordinate system about the helix axis.

(iii) Since the two planes which involve one adenine molecule each, the x',y',- and x'',y''-planes in Fig. 3, are inclined each other, it is not very easy to specify relative positions of the monomer transition moments by a polar coordinate fixed at each monomer position so as to fit the X-ray data. Instead, one can easily relate the components of these moments, $[\mu_{0\lambda}^{(m)}]\hat{\imath}$ *etc.*, to those described by the Cartesian coordinate system fixed at the adenine molecule (the X-axis is taken along the central C_4–C_5 bond, the X, Y-axes being in the molecular plane), specifying the following five angles as shown in Fig. 3 (let the plane perpendicular to the helix axis be the x,y-plane): An angle of rotation about the y-axis (*twist*); an angle of rotation about the x-axis (tilt); an angle between the x-axis and the original radial direction $\mathbf{r}$ $(\widehat{xr})$; an angle between the molecular X-axis and the radial direction $\mathbf{r}$ $(\widehat{Xr})$; an angle between the x'-axis and the radial direction $\mathbf{r}'$ on the x',y'-plane $(\widehat{x'r'})$. Values of the latter three angles are estimated from the observed values for the original x, y-plane.[11] A plus sign of the rotation angle is defined to be counterclockwise with respect to the right-handed coordinate system. Then we have

$$\begin{pmatrix} [\mu_{0\lambda}^{(1)}]_{\hat{\imath}} \\ [\mu_{0\lambda}^{(1)}]_{\hat{\jmath}} \\ [\mu_{0\lambda}^{(1)}]_{\hat{k}} \end{pmatrix} = \mathbf{R}_z(\widehat{xr})\cdot\mathbf{R}_y(-twist)\cdot\mathbf{R}_{x'}(-tilt)\cdot \mathbf{R}_{z'}(-\widehat{x'r'})\cdot\mathbf{R}_{z'}(\widehat{Xr}) \begin{pmatrix} [\mu_{0\lambda}^{(1)}]_X \\ [\mu_{0\lambda}^{(1)}]_Y \\ [\mu_{0\lambda}^{(1)}]_Z \end{pmatrix}, \tag{39}$$

where

$$\mathbf{R}_{x'}(-tilt) = \begin{pmatrix} 1 & 0 & 0 \\ 0 & \cos(-tilt) & \sin(-tilt) \\ 0 & -\sin(-tilt) & \cos(-tilt) \end{pmatrix}, \tag{40}$$

$$\mathbf{R}_y(-twist) = \begin{pmatrix} \cos(-twist) & 0 & -\sin(-twist) \\ 0 & 1 & 0 \\ \sin(-twist) & 0 & \cos(-twist) \end{pmatrix}, \tag{41}$$

and

$$\mathbf{R}_\zeta(Q) = \begin{pmatrix} \cos Q & \sin Q & 0 \\ -\sin Q & \cos Q & 0 \\ 0 & 0 & 1 \end{pmatrix} \tag{42}$$

for $\mathbf{R}_z(\widehat{xr})$, $\mathbf{R}_{z'}(-\widehat{x'r'})$, and $\mathbf{R}_{z'}(\widehat{Xr})$. These relationships are convenient for actual calculation of the polymer polarizability.

The transition moment of the second monomer can be related to that of the first one by

$$\mu_{0\lambda}^{(2)} = \mathbf{R}(180°)\cdot\mu_{0\lambda}^{(1)}, \tag{43}$$

where the definition of $\mathbf{R}(180°)$ follows Eq. 30.

Results and Discussion

The spectral parameters necessary for computations of the UV, ORD, and CD spectral bandshapes are listed in Table 1. These are the observed and/or assumed transition energies, oscillator strengths, damping factors, and directions of the transition moments of the adenine monomer. The damping factors are determined as described above so that a starting UV absorption bandshape function for adenine can reproduce roughly well the observed spectrum of adenine.

It is known experimentally that poly A in neutral solution takes a flexibly stacked conformation of single strand, while at low pH it becomes a protonated structure like

$$2(\text{poly A}) + 2H^+ \rightleftharpoons (\text{poly A}^+\text{H})\cdot(\text{poly A}^+\text{H}).$$

In this case, the base-pairing illustrated in Fig. 3 forms a rigid double-stranded helix (Fig. 1) for which we assume a parallelly interwound structure analyzed by Rich *et al.*;[11] pitch 3.8 Å at 45° rotation, a=2.97 Å, $tilt$=+4°, $twist$=+10°, $\widehat{Xr}$=−23.2°, $\widehat{x'r'}$=−117.4°. A number of model calculations are carried out by chang-

Table 1. Spectroscopic parameters for adenine taken from experimental data

pH	Energy[a] $hc\,\tilde{\nu}_{\lambda 0}^{(m)}$ (eV)	Oscillator strength $f_{\lambda 0}$	Damping[b] factor η_λ (eV)	Direction of transition moment[c] θ (°)
7	4.76	0.27[d]	0.184	+ 3
	5.99	0.40	0.158	−92
	6.53	0.26	0.184	+ 3
2.5	4.72	0.27[e]	0.187	+ 3
	6.18	0.26	0.119	−92
	6.51	0.40	0.236	+ 3

a) D. Voet, W. B. Gratzer, R. A. Cox, and P. Doty, *Biopolymers*, **1**, 193 (1963). b) Estimated from $hc\,\tilde{\nu}_{0\lambda}^{(m)}$, ε^M, and $f_{\lambda 0}$. The molar extinction coefficients, ε^M, are taken from a) above. c) A. F. Fucaloro and L. S. Forster, *J. Am. Chem. Soc.*, **93**, 6443 (1971); note that the signs are opposite to those of Fucaloro and Forster who follow the DeVoe-Tinoco convention. d) M. Tanaka and S. Nagakura, *Theor. Chim. Acta*, **6**, 320 (1966). e) Assumed from the UV absorption spectrum of adenine hydrochloride observed by H. H. Chen and L. B. Clark, *J. Chem. Phys.*, **58**, 2593 (1973).

Table 2. Figure index[a]

Fig. No.	Strand	*tilt* (°)	*twist* (°)	$\widehat{x'r'}$ (°)	Helix radius (Å)	*N*
4	Single	−4.0	0.0	0.0	2.97	2, 3, 8, 10, 12, 14
5	Single	4.0	10.0	−117.4	2.97, 5.0, 7.0	8
6	Single	−4.0	10.0	−27.4	2.97	8
		−2.0	0.0	−27.4	2.97	8
		4.0	10.0	−117.4	2.97	8
7[b]	Double	4.0	10.0	−117.4	2.97	8

a) Helical pitch: $L=3.8$Å, $\phi=45°$. $\widehat{Xr}=-23.2°$ is used for all calculations. b) $\gamma'=180°$.

ing values of the parameters from those for the reference structure cited above. In Table 2 are listed the values of these parameters and the figure numbers in which the predicted UV, ORD, and CD spectra are drawn. For convenience, it is assumed that the model for the single-stranded helix is not a flexibly and/or randomly stacked but has a regularly and rigidly stacked structure; in other words, it is regarded as a counterpart of the double helix (*vide infra*).

We show the bandshapes computed for the single-stranded poly A in Figs. 4—6 and those for the double-stranded poly A in Fig. 7. First of all, the effect of the chain-length (N) of the single-stranded poly A on bandshapes is examined in Fig. 4. Here we set $\widehat{x'r'}=0°$(*i.e.*, the *tilt* axis is taken along the radial direction and the *twist* axis along the tangential direction), *tilt*=−4.0°, and *twist*=0°. It is to be noted that a helical structure appears to begin even in the *dimer* ($N=2$) and *trimer* models ($N=3$), as can be seen in Fig. 4. With an increase of N, the UV, ORD, and CD bandshapes are likely to converge to respective certain shapes (Fig. 4), the trend being pointed out before by Tinoco *et al.* in the treatment of the exciton theory.[14] In comparison with the monomer UV bandshapes, a large hypochromism appears in the 260 nm region of all the polymer UV bandshapes in the pH 7 model calculations (Figs. 4—7), which is well compared with the UV absorption spectrum of poly A observed by Michelson,[15] and Beers and Steiner.[16] As for the ORD and CD bandshapes as well, the calculated curves are qualitatively in accord with those observed.[8-10]

The intensities of the ORD and CD spectra decrease and the UV bandshapes look like that of the free adenine molecule as the radius (a) of the helix increase, as can be seen in Fig. 5 where the X-ray data of the double-stranded poly A are used for the $N=8$ single-stranded poly A model calculations. The parameters, $\widehat{x'r'}=-27.4°$, *twist*=+10°, and *tilt*=−4°, in the $N=8$ model predict well the observed ORD[8], CD[9], and UV[10,15,16] spectral shapes (see Fig. 6), while the parameters taken from the X-ray data of the double-stranded poly A, $\widehat{x'r'}=-117.4°$, *twist*=+10°, and *tilt*=+4°, do not produce reasonable ORD and CD curves (a figure is not shown). This is particularly true for ORD and CD spectral features in the 230 nm region; the latter param-

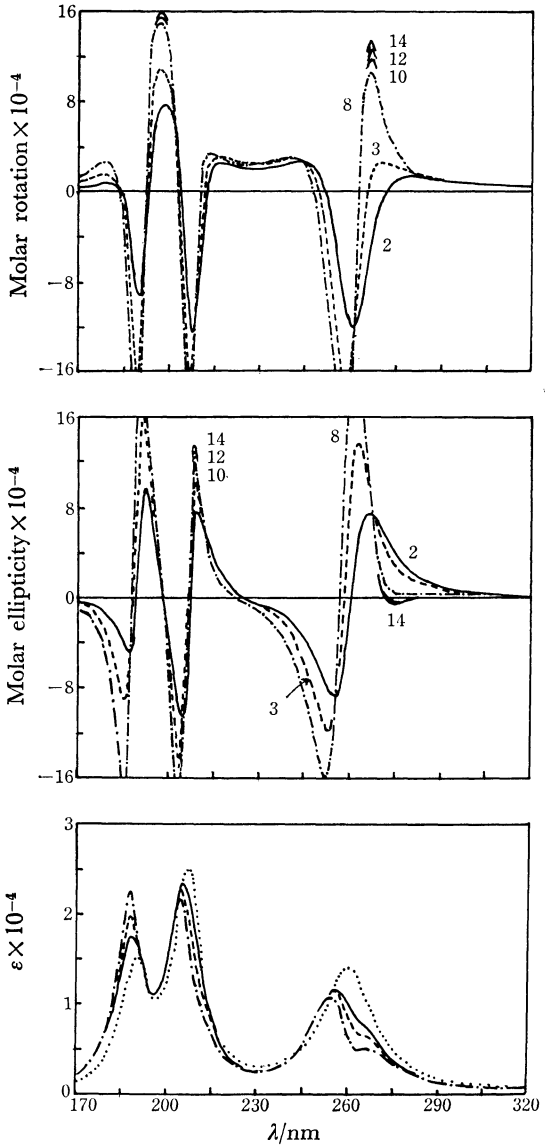

Fig. 4. The chain-length dependence ($N=2$, 3, 8, 10, 12, 14) of the ORD (top), CD (middle), and UV (bottom) bandshapes of the singlestranded polyadenylic acid ($a=2.97$Å, *tilt*=−4.0°, *twist*=0°, $\widehat{x'r}=0°$). The dotted line (·····) in the bottom shows the observed UV absorption spectrum of adenine.

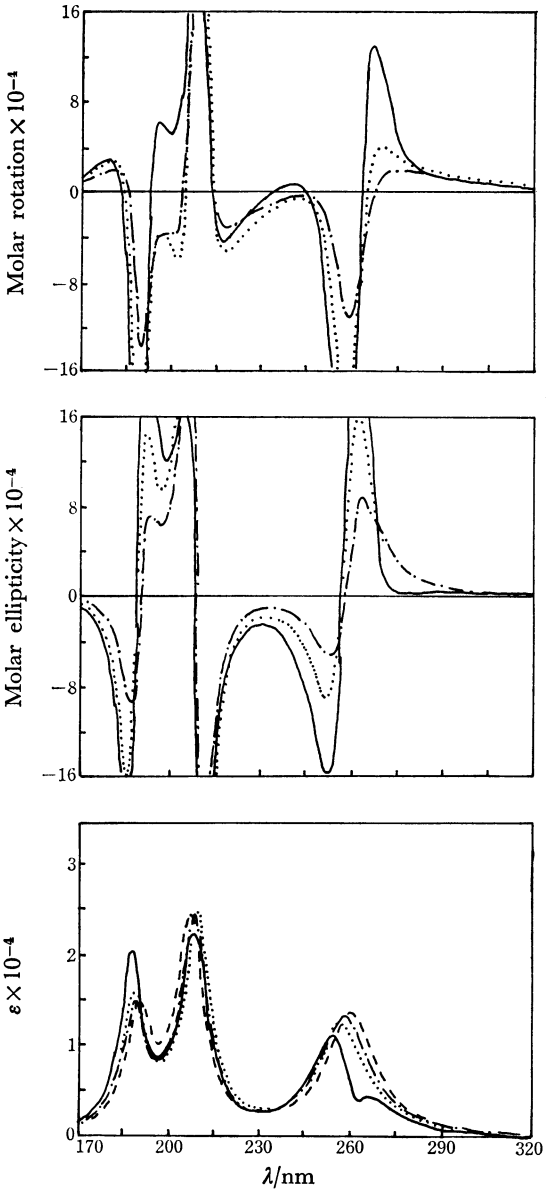

Fig. 5. Dependence of the ORD (top), CD (middle), and UV (bottom) bandshapes of the single-stranded polyadenylic acid on the radius (a) of the helix ($N=8$, $a=2.97$Å, $tilt=4°$, $twist=+10°$, $\widehat{Xr}=-23.2°$, $\widehat{x'r'}=-117.4°$). (——): $a=2.97$Å, (·····): $a=5.0$Å; (—·—): $a=7.0$Å. The broken line (- - -) in the bottom shows the observed UV absorption spectrum of adenine.

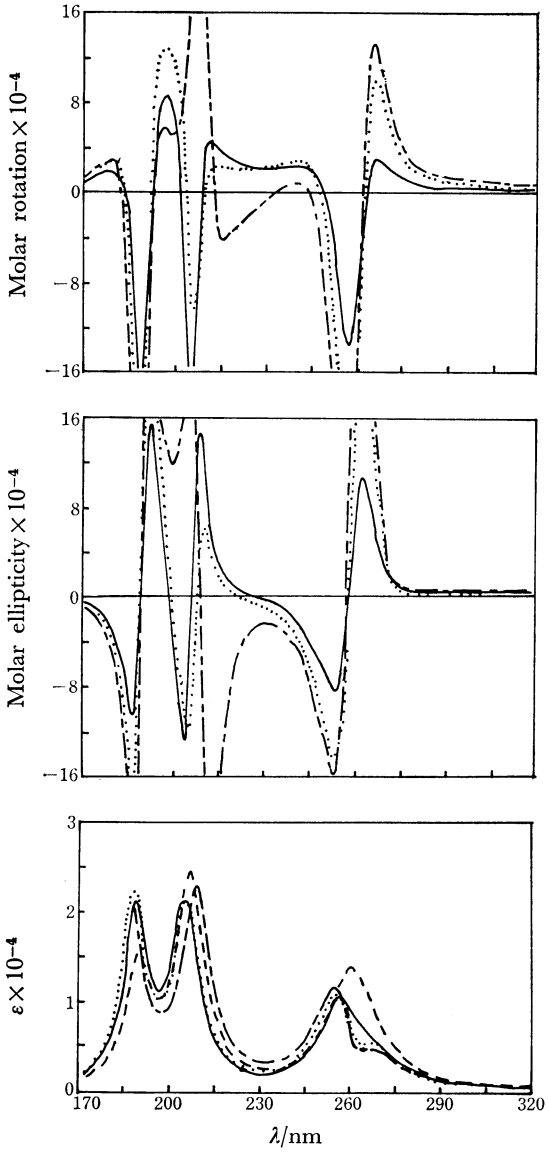

Fig. 6. Comparison of the selected theoretical ORD (top), CD (middle), and UV (bottom) bandshapes of the single-stranded polyadenylic acid in the $N=8$ model. (——): $tilt=-4°$, $twist=+10°$, $\widehat{x'r'}=-27.4°$; (·····): $tilt=-2°$, $twist=0°$, $\widehat{x'r'}=-27.4°$; (—·—): $tilt=+4°$, $twist=+10°$, $\widehat{x'r'}=-117.4°$. The broken line (- - -) in the bottom shows the observed UV absorption spectrum of adenine.

eters bring about a too small peak in the ORD 230 nm region and no positive peak in the CD 220 nm region. This is probably due to the assumption of the orderly arranged rigid structure for the single-stranded poly A which may be considered to have a considerably flexible structure in nature. The predicted ORD and CD curves are therefore slightly stronger in intensity at their peaks and troughs and the predicted UV spectral shapes show rather strong hypochromism, compared with the observed spectra to which rather loose conformations of poly A may contribute; the model can be considered to be in between the real single- and double-stranded poly A's.

In Fig. 7 are compared the bandshapes of the double-stranded poly A, one calculated with the spectral parameters for the pH 7 adenine and the other with those for the pH 2.5 adenine. This is because the ORD and CD spectra of the double-stranded poly A have been measured around pH 4.5, while the spectroscopic data for the pH 4.5 free adenine molecule are not available. The molecular geometries are taken from the X-ray data in either case. As a matter of course, the predicted UV, ORD, and CD spectral bandshapes markedly

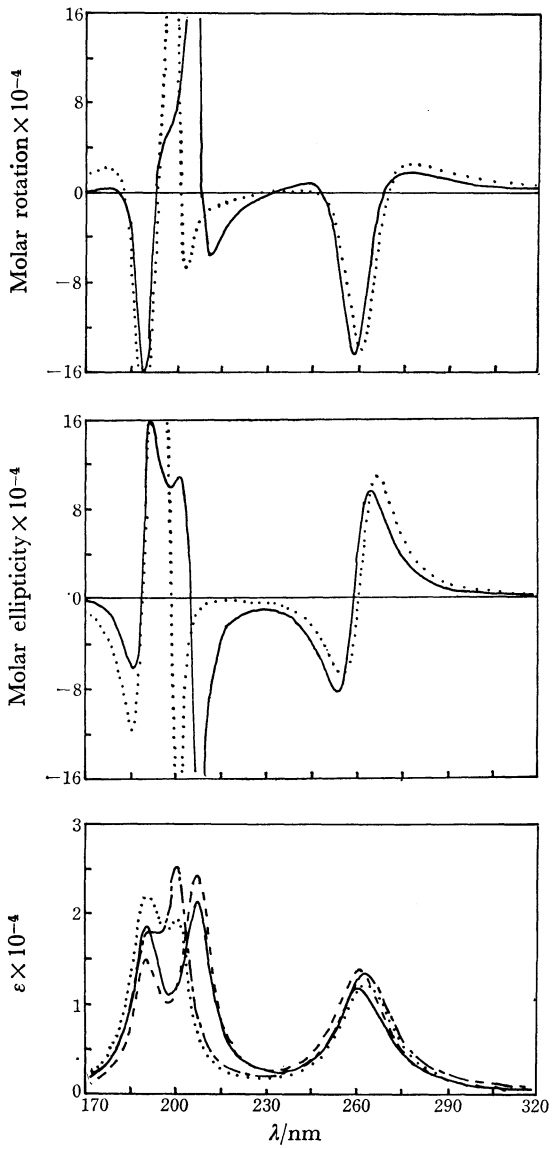

Fig. 7. Predicted ORD (top), CD (middle), and UV (bottom) bandshapes of the double-stranded polyadeylic acid ($N=8$, $a=2.97$Å, $titl=+4°$, $twist=+10°$, $\widehat{x'r'}=-117.4°$). (——): Calculated with the spectral parameters for pH=7 adenine; (·····): Calculated with the spectral parameters for pH=2.5 adenine. The broken line (- - -) in the bottom shows the observed UV absorption spectrum of adenine.

depend upon the pH values. In contrast with Fig. 6, the ORD and CD spectra turn out to be broader when the double-stranded helix is formed, which features agree in general with experiment.

Going into detail however, the predicted UV, ORD, and CD spectral intensities are in direct opposition to observations; in the observed spectra, the UV hypochromicity at the longer wavelength side enhances, and the ORD peak at 280 nm and the trough at 250 nm and the CD peak at 260 nm all gain their intensities at low pH, the CD trough at 240 nm being unchanged.

We now try to explain this discrepancy. The chain-length effect is notable as shown in Fig. 4, but it is to be recalled that a model for the single-stranded poly A adopted there corresponds to a counterpart of the double-stranded poly A. An actual structure of poly A in neutral solution is considered to be not so rigid as the present model but flexible to a certain extent. In fact, only small chain-length effect has been observed for poly A in neutral solution.[17] If we approximate a structure of poly A in the pH 7 solution as the dimer model ($N=2$ in Fig. 4), the relation between the UV hypochromicities and also the ORD and CD spectral intensities of the single- and double-stranded poly A's can be explained without difficulty. In other words, we may speculate that the structure of poly A in neutral solution is such that it can be approximated as an assembly of adenine dimer and/or trimer.

In alternative way of looking is possible. As Fig. 6 shows, the UV, ORD, and CD bandshapes of the single-stranded poly A approach those of free adenine as the position of the residues (a) gets away from the helix axis, simply because the relative distance between the two monomers located nearly on a level surface becomes larger and hence $\mathbf{U}_{mn}$ becomes smaller. Even when one does not throw over the rigid single-stranded model therefore, one only has to give larger values for a in order to get out of the above-mentioned dilemma.

An experimental fact must be mentioned to judge which view is right. Blake and Peacocke[18] observed a distinct Cotton effect around 440 nm due to proflavine bound to poly A in acid solution but no optical activity for the same system in neutral solution. This probably comes from the fact that in the poly A–proflavine complex the dyes are regularly arranged around the poly A double-helices in acid solution, while they are not because poly A does not take a regular helical structure in neutral solution.

The present treatment must await further improvements on quantitative description of spectral bandshapes of helical and non-helical biopolymers. We have not undertaken calculations with finer parametrization, since the spectral data available for the residue and the polymer in different pH solutions seem to be far from perfect. Nevertheless, we believe that the present theory and results provide a useful step for the understanding of the many-body aspect and the determination of conformations of helical biopolymers.

References

1) H. Ito, T. Eri, and Y. J. I'Haya, *Chem. Phys. Lett.*, **39**, 150 (1976); *ibid.*, **45**, 610 (1977).
2) U. Fano, *Phys. Rev.*, **118**, 451 (1960).
3) H. DeVoe, *J. Chem. Phys.*, **41**, 393 (1964).
4) H. DeVoe, *J. Chem. Phys.*, **43**, 3199 (1965).
5) A. Herzenberg and A. Modinos, *Proc. Phys. Soc.*, **87**, 597 (1966).
6) J. Applequist, *J. Chem. Phys.*, **58**, 4251 (1973).
7) C. L. Cech, W. Hug, and I. Tinoco, Jr., *Biopolymers*, **15**, 131 (1976).
8) D. N. Holcomb and I. Tinoco, Jr., *Biopolymers.*, **3**, 121 (1965).
9) J. Brahms, *Nature*, **202**, 797 (1964).
10) J. Brahms, A. M. Michelson, and K. E. Van Holde, *J. Mol. Biol.*, **15**, 467 (1966).

11) H. A. Rich, D. R. Davies, F. H. Crick, and J. D. Watson, *J. Mol. Biol.*, **3**, 71 (1961).
12) W. Kauzmann, "Quantum Chemistry," Academic Press, New York (1967), p. 579.
13) H. Ito, T. Eri, and Y. J. I'Haya, *Chem. Phys.*, **8**, 68 (1975); *ibid.*, **10**, 497 (1975).
14) I. Tinoco, Jr., R. W. Woody, and D. F. Bradle, *J. Chem. Phys.*, **38**, 1317 (1963).
15) A. M. Michelson, *J. Chem. Soc.*, **1959**, 1371.
16) R. F. Beers, Jr. and R. F. Steiner, *Nature*, **179**, 1076 (1957).
17) D. Poland, J. N. Vournakis, and H. A. Scheraga, *Biopolymers*, **4**, 223 (1966).
18) A. Blake and A. R. Peacocke, *Biopolymers*, **5**, 383 (1967).